Journal of Thermal Analysis and Calorimetry, Vol. 93 (2008) 2, 403–409

INVESTIGATION OF THERMAL BEHAVIOR OF NICOTINIC ACID

S. Jingyan[1], *L. Jie*[1], *D. Yun*[1], *H. Ling*[1], *Y. Xi*[1], *W. Zhiyong*[1], *L. Yuwen*[1,2*] *and W. Cunxin*[1]

[1]College of Chemistry and Molecular Science, Wuhan University, Wuhan 430072, China
[2]College of Life Science, Wuhan University, Wuhan 430072, China

The thermal behavior of nicotinic acid under inert conditions was investigated by TG, FTIR and TG/DSC-FTIR. The results of TG/DSC-FTIR and FTIR indicated that the thermal behavior of nicotinic acid can be divided into four stages: a solid-solid phase transition (176–198°C), the process of sublimation (198–232°C), melting (232–263°C) and evaporation (263–325°C) when experiment was performed at the heating rate of 20 K min^{-1}. The thermal analysis kinetic calculation of the second stage (sublimation) and the fourth stage (evaporation) were carried out respectively. Heating rates of 1, 1.5, 2 and 3 K min^{-1} were used to determine the sublimation kinetics.

The apparent activation energy, pre-exponential factor and the most probable model function were obtained by using the master plots method. The results indicated that sublimation process can be described by one-dimensional phase boundary reaction, $g(\alpha)=\alpha$. And the 'kinetic triplet' of evaporation process was also given at higher heating rates of 15, 20, 25, 30 and 35 K min^{-1}. Evaporation process can be described by model of nucleation and nucleus growing, $g(\alpha)=[-\ln(1-\alpha)]^{\frac{1}{3}}$.

Keywords: *evaporation, nicotinic acid, sublimation, TG-FTIR, thermal decomposition, thermogravimetry*

Introduction

Nicotinic acid (pyridine 3-carboxylic acid), which belongs to the B group of vitamins, is a beneficial compound for human and animal organism and plays an important role in several essential biochemical processes [1–4]. Nicotinic acid deficiency results in pellagra, affecting the gastrointestinal tract, skin and central nervous system. As an indispensable nutriment, it is used widely in many fields, such as food, forage, medicines, and cosmetics. In addition, it is also an important raw material and intermediate widely used in the syntheses of many medicines and dyes [5].

For the application of nicotinic acid, study of its thermal behaviors is urgently required. The thermal induced processes of nicotinic acid have been reported in previous literatures [6–9], but for some reasons, it is so far to describe the thermal processes in details. Vora *et al*. [9] suggested that after a solid-solid state phase transition, a dual sublimation and evaporation phase was followed. While Wang *et al.* [7] considered that the last stage was the melting of nicotinic acid and decomposition. So the aim of this work is to investigate thoroughly the thermal processes of nicotinic acid and ascertain the mechanism. For this purpose, the TG-FTIR technique, which can conduct simultaneous and continuous real time analysis [10–17], is used. It can provide more information about the reaction sequences and the relevant products.

In addition, little information on the kinetic aspects of these processes has been reported in previous literatures. Vora [9] has done kinetic studies of these processes by single heating rate method, which is considered unreliable now. In present work, multiple heating rate method has been used. The 'kinetic triple': apparent activation energy, pre-exponential factor and the most probable model function of both sublimation and evaporation processes were obtained by the isoconversional method and the master plots method, respectively.

Theoretical

For a reaction under non-isothermal condition, its kinetic function can be described as the following form:

$$g(\alpha)=\frac{AE_a}{\beta R}P(u) \qquad (1)$$

where α is the extent of conversion, β the heating rate, E_a the apparent activation energy, R the gas constant, A the pre-exponential factor, $g(\alpha)$ is the integral expression of kinetic model function, and $P(u)=\int_{\infty}^{n}-(e^u/u^2)du$, $u=E_a/RT$.

Because the exponential integral, has no analytical solution, an approximation formula of high accuracy [18] was used.

* Author for correspondnce: ipc@whu.edu.cn

1388–6150/$20.00

Akadémiai Kiadó, Budapest, Hungary
Springer, Dordrecht, The Netherlands

$$-\ln P(u)=0.37773896+1.89466100\ln u + \\ +1.00145033u \quad (2)$$

Inserting Eq. (2) into Eq. (1), one can obtain:

$$\ln\left[\frac{\beta}{T^{1.894466100}}\right]= \\ \left[\ln\frac{AE_a}{Rg(\alpha)}+3.63504095-1.89466100\ln E_a\right]- \\ -1.00145033\frac{E_a}{RT} \quad (3)$$

The first term at the right side of Eq. (3) is a constant corresponding to a given value of α. So for a series of experiments at different heating rates, the plot of $\ln(\beta/T^{1.89466100})$ *vs.* $1/T$ with the same conversional ratio should be a line with the slope of –1.00145033 E_a/R. Then, the apparent activation energy E_a can be calculated from the slope regardless of reaction mechanism.

Substituting α=0.5 into Eq. (1) results in the following equation:

$$g(0.5)=\frac{AE_a}{\beta R}P(u_{0.5}) \quad (4)$$

where $u_{0.5}=E_a/RT_{0.5}$, $T_{0.5}$ is the temperature when α is equal to 0.5.

With Eq. (1) and Eq. (4), we can arrive at the equation:

$$\frac{g(\alpha)}{g(0.5)}=\frac{P(u)}{P(u_{0.5})} \quad (5)$$

By plotting $g(\alpha)/g(0.5)$ *vs.* α according to different theoretical model functions, the theoretical master plots can be obtained for different kinetic mechanisms. With E_a calculated from Eq. (3), the experimental master plots of $P(u)/P(u_{0.5})$ *vs.* α could be drawn from the experimental data obtained under different heating rates. Equation (5) indicates that, for any given α, the experimental value of $P(u)/P(u_{0.5})$ and theoretically calculated value of $g(\alpha)/g(0.5)$ are equivalent when an appropriate kinetic model is used. So this integral master plots method can be used to determine the reaction kinetic models of non-isothermal reactions.

Then, the pre-exponential factor A can be estimated from the slope of the plot of g(α) *vs.* $E_aP(u)/\beta R$.

Experimental

Commercially available nicotinic acid (Analytical Grade, Duchefa) was used without further purification.

TG measurements were performed on a Setaram Setsys 16 TG-DTG/DSC Instrument, France. Instrument calibration was performed with standard indium, tin, lead, zinc, silver and gold samples of known melting temperature. All standards were of purity >99.99%. For the kinetics measurements, about 5 mg sample was weighted into an open alumina crucible. The furnace temperature was programmed to rise from ambient temperature to 400°C linearly at the rates of 1, 1.5, 2, 3, 15, 20, 25, 30, 35 K min^{-1}. The reaction atmosphere was nitrogen gas of high purity (≥99.999%) with a flow rate of 50 mL min^{-1}.

The TG-FTIR system composed of the Setaram Setsys 16 TG-DTA/DSC Instrument and a Thermo Nicolet Nexus 670 Fourier Transform Infrared Spectrometer. For TG-FTIR measuring, about 10 mg sample was weighted into an open alumina crucible. The heating rate of the TG furnace was 20 K min^{-1}, and nitrogen gas of high purity (≥99.999%) with a flow rate of 100 mL min^{-1} was used as carrier gas. The sample was heated from ambient temperature to 400°C. The transfer line used to connect TG and FTIR was a 1 m long stainless steel tube with an internal diameter of 2 mm. The TG accessory of the IR Spectrometer was used, in which has a 45 mL gas cell with a 200 mm path length. Both the transfer line and the gas cell were kept at a constant temperature of 200°C. The IR spectra were collected at 8 cm^{-1} resolution, co-adding 8 scans per spectrum. This resulted in a temporal resolution of 4.32 s. Lag time that the gas products went from furnace to gas cell was about 7 s. The FTIR spectra have been identified based on the FTIR reference spectra available on the World Wide Web in the public spectrum libraries of NIST [19].

FTIR measurements of the pure nicotinic acid and its solid condensate after heated in a tube full of N_2 were carried out with a Thermo Nicolet 360 Fourier Transform Infrared Spectrometer. The data was collected at a resolution of 4 cm^{-1} in the range 4000–400 cm^{-1} using KBr pellet technique.

Results and discussion

The thermal behavior of nicotinic acid

With consideration of the lag time from furnace to gas cell, TG/DSC-FTIR curves corresponding to the thermal behavior of nicotinic acid at the heating rates 20 K min^{-1} were shown in Fig. 1. The TG curve in Fig. 1 indicated that the thermal behavior of nicotinic acid was characterized by a single stage with mass percent loss (mass%) of almost 100% at 176–350°C. But DSC curve exhibited three endothermic peaks with the peak temperature 183.89, 242.36 and 296.95°C respectively. The first peak was assigned to the solid-solid phase transition, the second one

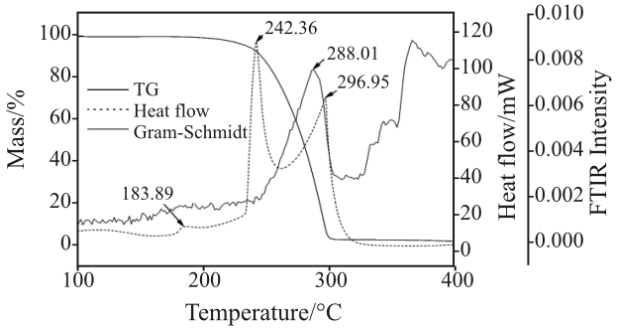

Fig. 1 The curves of TG, Heatflow and the Gram-Schmidt of evolved gases at heating rate of 20 K min^{-1}, N_2 flow rate 100 mL min^{-1}

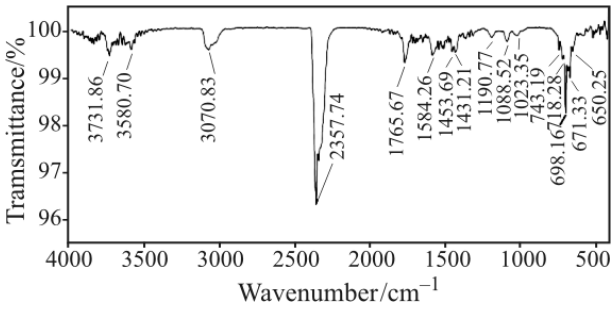

Fig. 2 FTIR spectrum of evolved gases from nicotinic acid decomposed in N_2, measured at 288.01°C by online-coupled TG-FTIR (heating rate 20 K min^{-1}; N_2 flow rate 100 mL min^{-1})

corresponded mainly to the melting of nicotinic acid, and the third one may be caused by evaporation or decomposition [7, 9]. Gram-Schmidt curve indicated that the gaseous products began to be evolved at 245°C, and reached their maximum releasing rate at 288.01°C, which coincided with the TG curve. And the IR absorbance after 325°C, which happened after 100% mass loss, was considered caused by the condensates attached to the transfer pipeline.

A typical spectrum obtained at 288.01°C was shown in Fig. 2. From Fig. 2, three species, nicotinic acid, CO_2 and pyridine were identified. Carbon dioxide was confirmed by the characteristic peaks at 2358 and 671 cm^{-1}. The existence of nicotinic acid can be ascertained by the characteristic peaks: υ_{O-H} 3581 cm^{-1}, $\upsilon_{=C-H}$ 3071 cm^{-1}, $\upsilon_{C=O}$ 1766 cm^{-1}, $\upsilon_{C=C}$ 1584–1431 cm^{-1}, $\delta_{=C-H}$ (in-plane) 1191–1023 cm^{-1}, $\delta_{=C-H}$ (out-of-plane) 743–600 cm^{-1}. Though IR absorbance of pyridine overlaps with that of nicotinic acid, pyridine can still be identified by absorption peak in the fingerprint region at 698.16 cm^{-1}. In addition, with consideration of the existence of CO_2, it was not difficult to deduce the existence of pyridine as another product of decomposition

According to above results, the decarboxylating is the only step in thermal decomposition of nicotinic acid below 400°C. And the existence of nicotinic acid in evolved gases suggested that the physical process, sublimation or evaporation, was also the reason for mass loss.

The IR absorption spectra of the evolved gases at different temperature were shown in Fig. 3. From Fig. 3, it can be observed that three gaseous products appeared and reached their maximum evolution rate simultaneously. Moreover, Fig. 3 showed that all these IR absorbance was very weak. For CO_2 and pyridine, as the easily volatile products, their weak IR absorbance indicated their low concentrations. And this suggested that the quantity of nicotinic acid decomposed was very minor. While for nicotinic acid, due to its high boiling point, most of them were condensed in the transfer pipeline, which also resulted in its weak IR absorbance. These suggested that the phase transitions, sublimation and evaporation, rather than decomposition were the main cause for mass loss. To ensure this, we carried out the following experiment.

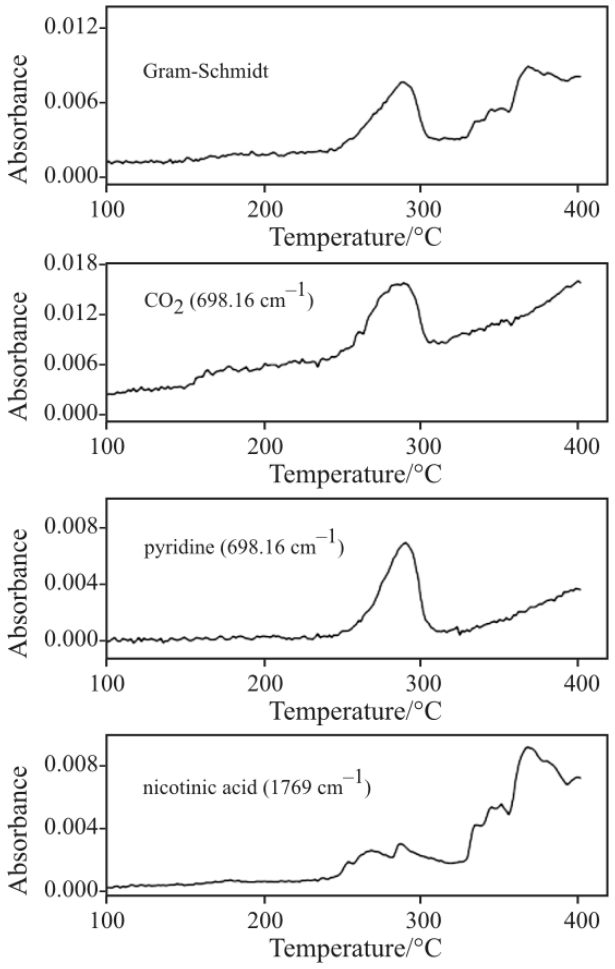

Fig. 3 Absorbance at different wavenumbers *vs.* temperature curves of evolved gases from nicotinic acid decomposed in N_2, measured by online-coupled TG-FTIR (heating rate 20 K min^{-1}; N_2 flow rate 100 mL min^{-1})

About 0.4 g nicotinic acid was heated in a tube full of N_2. The pledget was placed on the tube nozzle to avoid the overflow of products from the tube. At first some white product appeared and was cooled on the wall, then the sample began to melting, subsequently more condensates appeared on the wall. When no remnant was left at the bottom, heating ceased. After experiment, the tube was weighed again and it was found that more than 98% (in mass) recovery of condensates was obtained. Both the collected condensates and pure nicotinic acid were investigated by FTIR, and the results were shown in Fig. 4. Figure 4 showed that the IR spectrum of the solid condensate was the same as that of pure nicotinic acid. This indicated that the condensates were nicotinic acid.

Therefore, it can be concluded that the thermal induced processes of nicotinic acid belongs mainly to physical changes when heated. With consideration of the little mass change (less than 2%) after heated and the weak IR intensity of the evolved gases from the Gram–Schmidt curve in Fig. 3, we believed that the mass loss caused by decomposition was less than sublimation and/or evaporation.

In a word, the thermal induced processes of nicotinic acid can be divided into four stages (Fig. 5) at the heating rate of 20 K min^{-1}: (1) the first stage (176–198°C) is the solid-solid phase transition, in which no mass loss was observed on the TG curve; (2) the second stage (198–232°C) is the subliming, in which about 3.48% mass loss was observed on the TG curve. This stage happened below the melting point (236.6°C [20]) of nicotinic acid and no decomposition product was observed on the Gram–Schmidt curve; (3) the third stage (232–263°C) is the melting, accompanying subliming and evaporation; and (4) the fourth stage (263–325°C) is the evaporation.

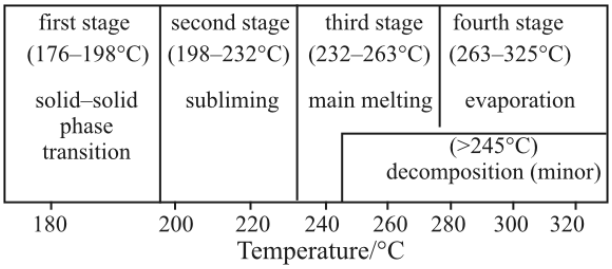

Fig. 5 Four stages of thermal behavior of nicotinic acid at the heating rate of 20 K min^{-1}

The thermal kinetics analysis of nicotinic acid

To clarify the processes of the thermal behavior of nicotinic acid, we calculated the activation energy with TG data over the α range from 0.1–0.9 with an increment of 0.02 at the heating rates of 15, 20, 25, 30 and 35 K min^{-1} by the isoconversional method, and the result was shown in Fig. 6. From Fig. 6, it can be observed that the activation energy took on two plateaus over the α ranges from 0.1–0.2 and 0.4–0.9, which indicated that the whole process included two steps and each of them may obey single-step reaction mechanism. Combining with the results of mechanism analysis, the first plateau should be corresponded to the sublimation of nicotinic acid and the second should be corresponded to the evaporation process.

To analysis the kinetics of sublimation and evaporation processes more precisely, we choose different heating rate ranges for these two processes. As to sublimation, lower heating rates (1–3 K min^{-1}) were

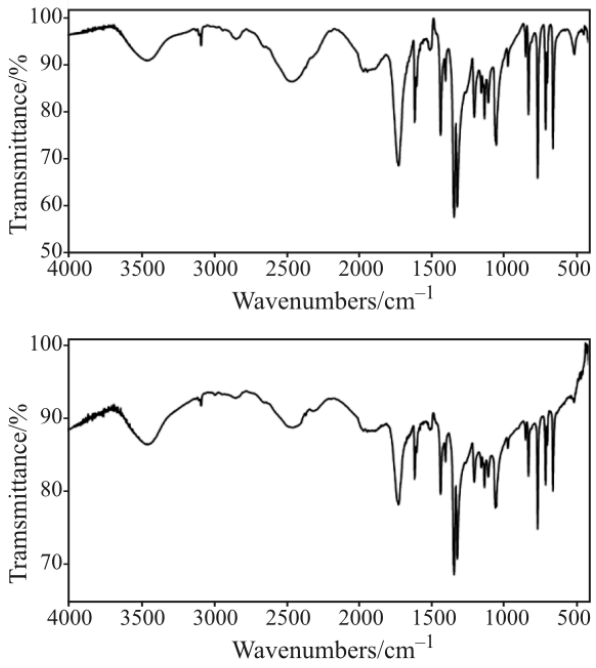

Fig. 4 a – FTIR spectrum of pure nicotinic acid; b – solid condensate

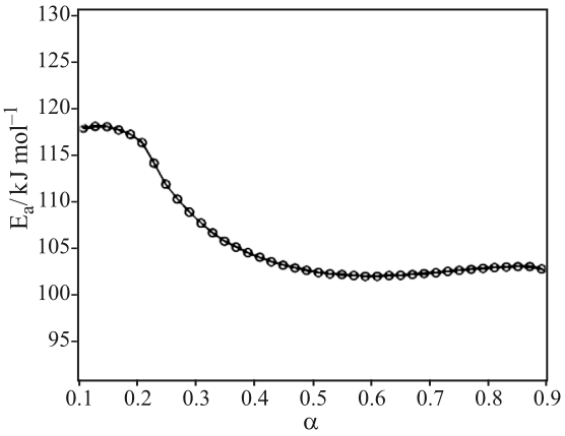

Fig. 6 The activation energy of whole process at the heating rates of (15, 20, 25, 30, 35 K min^{-1})

adopted to avoid the effects of melting and evaporation. While for evaporation, higher heating rates (15–35 K min^{-1}) were used.

The thermal kinetics analysis of subliming process at lower heating rates

The heating rates of 1, 1.5, 2 and 3 K min^{-1} were selected to study the sublimation process. Because with low heating rates, almost 100% mass loss had taken place below the melting point of nicotinic acid. So the mass loss in this stage should be caused mainly by sublimation. And the effects of processes such as evaporation and decomposition on the mass loss can be neglected. TG curves at four lower heating rates 1, 1.5, 2 and 3 K min^{-1} were shown in Fig. 7. The values of α among 0.1–0.9 with an increment of 0.05 were chosen for kinetic calculation. Plotting $\ln(\beta/T^{1.89466100})$ *vs.* $1/T$ using a linear regressive of least-square method, we got the values of E_a at different conversions which were listed in Table 1. As shown in Table 1, all the plots had linear correlation coefficients larger than 0.99. The apparent activation energy did not vary with the increase of conversion ratios and the average value is 105.09±0.48 kJ mol^{-1}. Little dependence of the activation energy on the extent of conversion suggests that the reaction took place through a single-step reaction mechanism.

Table 1 The apparent activation energy E_a and the correlation coefficients r of linear r regression at different conversion ratios α

α	E_a/kJ mol^{-1}	r
0.10	106.54	0.9970
0.15	105.85	0.9967
0.20	105.00	0.9975
0.25	104.65	0.9977
0.30	104.73	0.9976
0.35	104.78	0.9974
0.40	104.97	0.9976
0.45	104.81	0.9979
0.50	104.68	0.9982
0.55	104.77	0.9984
0.60	105.02	0.9984
0.65	105.20	0.9984
0.70	105.27	0.9983
0.75	105.30	0.9983
0.80	105.28	0.9983
0.85	105.03	0.9982
0.90	105.70	0.9982
Average E_a=105.09±0.48		

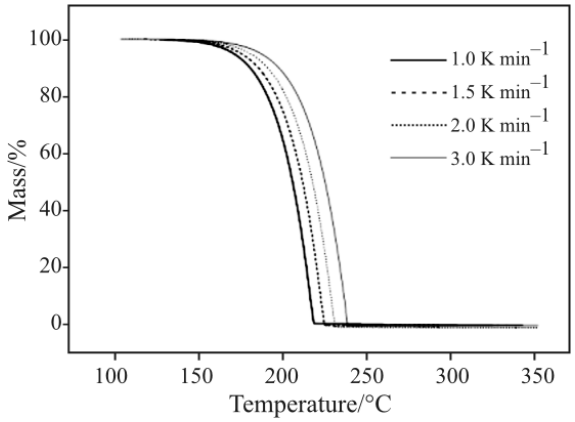

Fig. 7 TG curves of nicotinic acid at lower heating rates, N_2 flow rate 50 mL min^{-1}

To determine the most probable mechanism, 40 basic model functions [21] were tested. According to the value of E_a, the theoretical master plots of $g(\alpha)/g(0.5)$ *vs.* α and the experimental master plots of $P(u)/P(u_{0.5})$ *vs.* α were obtained, as shown in Fig. 8. The superposition of experiment master plots at different heating rates indicated that the kinetics process of thermal mass loss of nicotinic acid can be described by a single model function. It can be easily seen from Fig. 8 that the most probable model function is the No. 26 function, $g(\alpha)=\alpha$, which is used to describe one-dimensional phase boundary reaction. As we know, this model describes reaction whose rate is proportional to the surface area of interface. And it is often used to describe the sublimation process [21].

By plotting $g(\alpha)$ *vs.* $E_aP(u)/\beta R$ at different heating rate (shown in Fig. 9), the pre-exponential factor $\ln A$=18.83±0.02 was obtained. In Fig. 9 the slope of the plots represented the pre-exponential factor, so these parallel straight lines indicated that

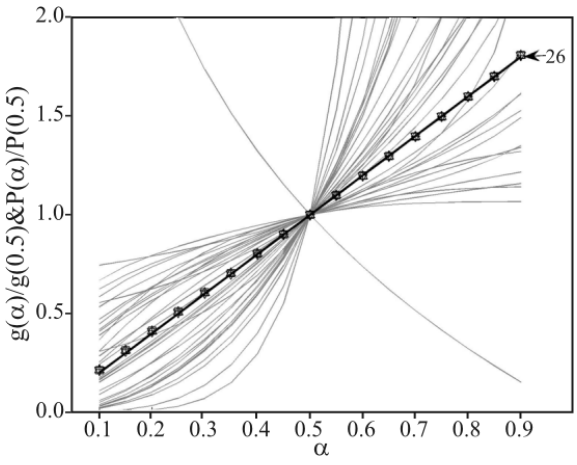

Fig. 8 —–The theoretical master plots and the experimental master plots at heating rates of + – 1, ▽– 1.5, △ – 2 and □ – 3 K min^{-1}. The highlighted plot represents the most probable model function (No. 26)

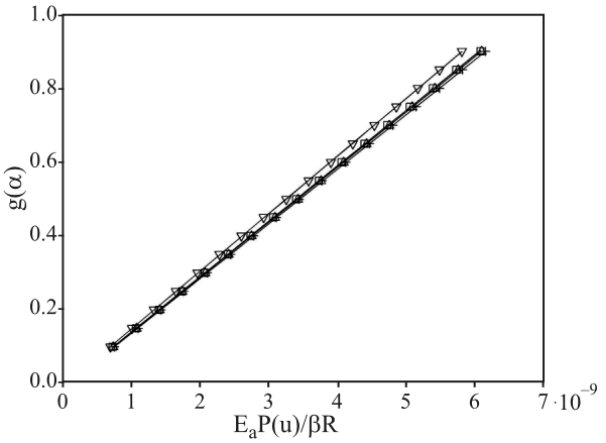

Fig. 9 The curves of $g(\alpha)$ *vs.* $E_aP(u)/\beta R$ at the heating rate of + – 1, ▽– 1.5, △ – 2 and □ – 3 K min^{-1}; —·– the result of linear fitting

the value of pre-exponential factor obtained from different heating rate was in good agreement with each other. And the slight departure of the plot at heating rate of 1.5 K min^{-1} was caused by the experimental error.

The thermal kinetics analysis of evaporation process at higher heating rates

The reason for using the heating rates of 15, 20, 25, 30 and 35 K min^{-1} to investigate the evaporation is that with higher heating rates, evaporation should be more important as a cause of mass loss in the last stage. TG curves corresponding to the thermal behaviors of nicotinic acid at the higher heating rates were shown in Fig. 10. With the same method, the kinetic calculation of evaporation process was performed by using the data from the fourth stage. The results were shown in Table 2 and Figs. 11, 12. The apparent activation energy was 102.33±0.41 kJ mol^{-1} with good linear correlation coefficients. And from Table 2, it can be easily seen that the apparent activation energy had little dependence on the extent of conversion, which indicated that the evaporation process can be described by single-step reaction mechanism. Figure 11 indicated that the most probable model function was the No. 11 function, $g(\alpha)=\left[-\ln(1-\alpha)\right]^{\frac{1}{3}}$, which was a model of nucleation and nucleus growing. It was often used to describe the process of formation of a new phase in a heterogeneous medium [22]. The evaporation process of nicotinic acid was coincident with the process described by No. 11 function. By plotting $g(\alpha)$ *vs.* $E_aP(u)/\beta R$ at different heating rate (shown in Fig. 12), the pre-exponential factor $\ln A$=18.60±0.04 was obtained.

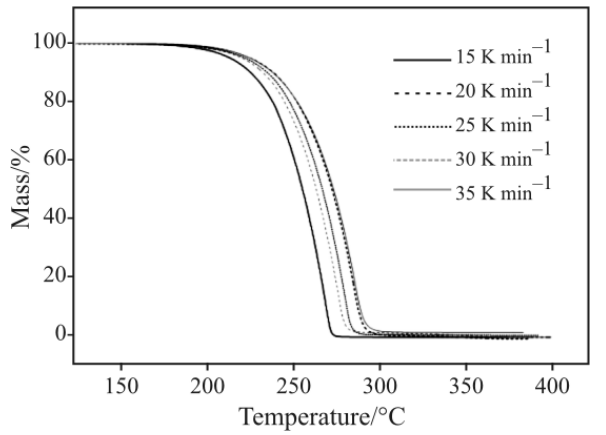

Fig. 10 TG curves of nicotinic acid at different heating rates, N_2 flow rate 50 mL min^{-1}

Table 2 The apparent activation energy E_a and the correlation coefficients r of linear regression at different conversion ratios α at high heating rates for the last stage

α	E_a/kJ mol^{-1}	r
0.20	102.13	0.9900
0.25	101.97	0.9904
0.30	101.86	0.9906
0.35	101.84	0.9908
0.40	101.93	0.9910
0.45	102.05	0.9912
0.50	102.19	0.9913
0.55	102.40	0.9914
0.60	102.57	0.9915
0.65	102.72	0.9915
0.70	102.86	0.9915
0.75	102.94	0.9914
0.80	102.83	0.9914
Average E_a=102.33±0.41		

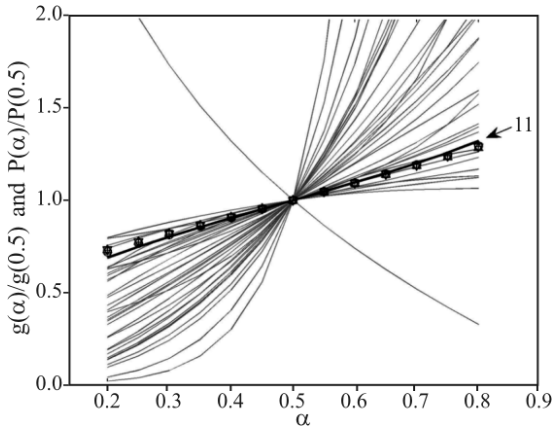

Fig. 11 —·– The theoretical master plots and the experimental master plots at heating rates of + – 15, ▽ – 20, △ – 25, □ – 30 and ○ – 35 K min^{-1}. The highlighted plot represents the most probable model function (No. 11)

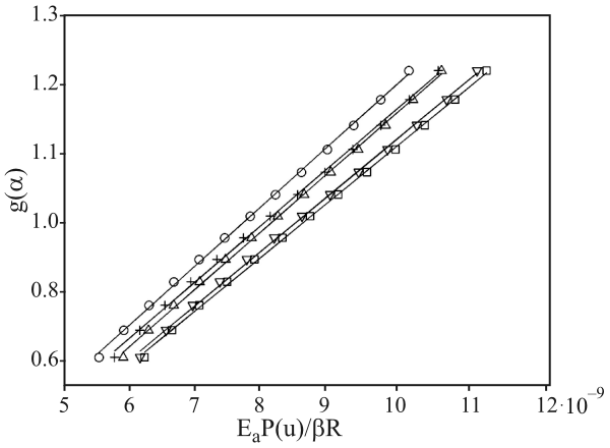

Fig. 12 The curves of $g(\alpha)$ *vs.* $E_aP(u)/\beta R$ at the heating rate of + – 15, ▽ – 20, △ – 25, □ – 30 and ○ – 35 K min^{-1}; — – the result of linear fitting

Conclusions

The thermal behavior of nicotinic acid is discussed in details. By TG, FTIR and TG/DSC-FTIR, four stages were suggested: solid–solid phase transition, subliming, melting and evaporation. And the decomposition is a less important cause for the mass loss in the whole process.

The thermal analysis 'kinetic triplet' of sublimation and evaporation processes were obtained by the isoconversional method and the master plots method, respectively. This method belongs to the method of multiple heating rates, which has higher accuracy than single heating rate in dealing with the kinetic calculation. By this method, the activation energy E_a can be obtained regardless of reaction mechanism, which is considered more reliable. And in present work, the most probable model functions: one-dimensional phase boundary reaction function (R1) and Avrami–Erofeev function (A3) can give the adequate kinetic descriptions for the sublimation and evaporation processes, respectively.

On the other hand, the experimental results showed that the heating rate had great effect on the thermal behavior of nicotinic acid. Certain process can be thoroughly investigated by choosing appropriate heating rates.

Acknowledgements

This work was financially supported by the National Nature Sciences Foundation of China (Grant No. 20373050, 30600116), Nature Sciences Foundation of Hubei and China Postdoctoral Science Foundation.

References

1 T. M. Delvin Ed., Textbook of Biochemistry with Clinical Correlations, Wiley, New York, 1992, p. 135.
2 R. S. Rosenson, Atherosclerosis, 171 (2003) 87.
3 B. Müller, M. Kasper, Ch. Surber and G. Imanidis, Eur. J. Pharm. Sci., 20 (2003) 181.
4 T. A. Ban, Prog. Neuro-Psychoph., 25 (2001) 709.
5 D.-Z. Liu, K.-Y. Gao and L.-B. Cheng, Dyes and Pigments, 33 (1997) 87.
6 D.Menon, D. Dollimore and K. S. Alexander, Thermochim. Acta, 392–393 (2002) 237.
7 S.-X. Wang, Z.-C. Tan, Y.-Y. Di, F. Xu, M.-H. Wang, L.-X. Sun and T. Zhang, J. Therm. Anal. Cal., 76 (2004) 335.
8 A. Moussaoui, A. Chauvet and J. Masse, J. Thermal Anal., 39 (1993) 619.
9 P. Vora, D. Menon, M. Samtani, D. Dollimore and K. Alexander, Instrum. Sci. Technol., 29 (2001) 231.
10 W. Xie and W.-P. Pan, J. Therm. Anal. Cal., 65 (2001) 669.
11 K. Marsanich, F. Barontini, V. Cozzani and L. Petarca, Thermochim. Acta, 390 (2002) 153.
12 M. Webb, P. M. Last and C. Breen, Thermochim. Acta, 326 (1999) 151.
13 C. Breen, P. M. Last, S. Taylor and P. Komadel, Thermochim. Acta, 363 (2000) 93.
14 W. M. Groenewoud and W. de Jong, Thermochim. Acta, 286 (1996) 341.
15 A. Marcilla, M. I. Beltran and R. Navarro, J. Therm. Anal. Cal., 87 (2007) 325.
16 T. Kaljuvee, J. Pelt and M. Radin, J. Therm. Anal. Cal., 78 (2004) 399.
17 J. Li, Z.-Y. Wang, X. Yang, L. Hu, Y.-W. Liu and C.-X. Wang, J. Anal. Appl. Pyrolysis, 80 (2007) 247.
18 W.-J. Tang, Y.-W. Liu, H. Zhang and C.-X. Wang, Thermochim. Acta, 408 (2003) 39.
19 NIST Chemistry Webbook Standard Reference Database No. 69, June 2005 Release (http://webbook.nidt.gov/chemistry).
20 C. O. Wilson, O. Gisvold and R. F. Doerge, Eds., Textbook of Organic Medicinal and Pharmaceutical Chemistry, J. B. Lippinocott, PA, 1977, p. 917.
21 J. Li, Z.-Y. Wang, X. Yang, L. Hu, Y.-W. Liu and C.-X. Wang, Thermochim. Acta, 447 (2006) 147.
22 V. Mamleev, S. Bourbigot, M. L. Bras, S. Duquesne and J. Šesták, Phys. Chem. Chem. Phys., 2 (2000), 4708.

Received: June 7, 2007
Accepted: October 12, 2007

DOI: 10.1007/s10973-007-8593-7